Journal of Basic and Applied Engineering Research
p-ISSN: 2350-0077; e-ISSN: 2350-0255; Volume 6, Issue 2; January-March, 2019, pp. 113-121

http://www.krishisanskriti.org/Publication.html

Numerical Investigation on Natural Convection in a Sinusoidal Corrugated Inclined Enclosure Due to Effects of a Longitudinal Magnetic Field

Pravez Alam[1] and S. Kapoor[2]

[1]Department of Mathematics, H.N.B Garhwal Central University, Srinagar 246174, India
[2]Department of Education in Science and Mathematics, Regional Institute of Education (NCERT), Bhubaneswar 751022, India
E-mail: [1]alampr09@gmail.com

Abstract—*A comprehensive numerical investigation on the natural convection in a tilted sinusoidal corrugated inclined enclosure due to effects of a longitudinal magnetic field is presented. In this analysis, two sinusoidal corrugated side walls are maintained at a constant low temperature whereas a constant heat flux source whose length is varied from 20% to 80% of the total length of the enclosure is discretely embedded at the bottom wall. The finite element method has been used to solve the governing differential equations of the fluid medium in the enclosure in order to investigate the effects of the variation of inclination angles, the presence of a longitudinal magnetic field and different discrete heat source size ratios on heat transfer process for different values of Rayleigh and Hartmann numbers. Results are presented in the form of streamline as well as temperature profile. It is concluded that the average Nusselt number increases as the heat surface length decreases, while the enclosure inclination angle has a clear effect on the heat transfer process for low heat source lengths in case of low buoyancy and magnetic effects. The dominance of Hartmann number is found to be significant with the purpose of reducing heat transfer process as well as minimizing the influence of inclination angles at low Rayleigh number.*

Keywords*: MHD natural convection, longitudinal magnetic field, corrugated enclosure, Hartmann number.*

Nomenclature

B_o	magnitude of the magnetic field [T]
g	gravitational acceleration [ms^{-2}]
Ha	Hartmann number
k	thermal conductivity of fluid [$Wm^{-1}K^{-1}$]
L	length of the heat source [m]
Nu	average Nusselt number
p	pressure [Nm^{-2}]
P	dimensionless pressure
Pr	Prandtl number
q	heat flux [Wm^{-2}]
Ra	Rayleigh Number
T	temperature [K]
T_c	temperature of the cold surface (K)
u, v	velocity components in x and y-direction [ms^{-1}]
U, V	dimensionless velocity components in X, Y-direction
W	length of the enclosure [m]
x, y	Cartesian co-ordinates [m]
X, Y	dimensionless Cartesian co-ordinates
Greek symbols	
α	thermal diffusivity [m^2s^{-1}]
β	coefficient of volumetric thermal expansion [K^{-1}]
ε	discrete heat source size ratio
θ	dimensionless temperature
μ	dynamic viscosity of fluid [$kgm^{-1}s^{-1}$]

ρ density of fluid [kgm^{-3}]
σ_e electric conductivity [Sm^{-1}]
υ kinematic viscosity of fluid [m^2s^{-1}]
Φ inclination angle [deg]

1. INTRODUCTION

The application of a magnetic field in various research areas has significantly increased in recent years. The development of super-conducting magnets has allowed the generation of magnetic fields up to 20 T (or higher with hybrid magnets) as reported by Teamah [1]. However, due to the development of superconducting magnets, a new phenomenon called magnetic convection could be investigated. Braithwaite *et al.* [2] was the first researcher reported the influence of magnetic field on the natural convection of a paramagnetic fluid. Many investigators studied the simple rectangular and square cavities with temperature gradient experimentally and numerically. A good review was reported by Ostrach [3]. Ozoe and Okada [4] conducted a numerical analysis of the magnetic damping effect in a cubic cavity with two vertical walls at different temperatures. They found that the strongest damping effect was achieved with the magnetic field applied perpendicular to the hot wall. Tagawa *et al.* [5] employed a similar way to Boussinesq approximation for the magnetic force and carried out numerical analysis for natural convection of air in a cubic enclosure. Kaneda *et al.* [6] studied natural convection in a cubic enclosure filled with air. The cube was heated from above and cooled from bottom and the air was driven by a magnetic force. Experimental investigation of the thermally induced convection of molten gallium in magnetic fields was carried out by Xu *et al.* [7]. Seki *et al.* [8] studied the laminar natural convection of mercury subjected to a magnetic field parallel to gravity in a rectangular enclosure. Numerical results were found and compared to their experiment with which considered a partially heated vertical wall by a uniform heat generator. Rudraiah *et al.* [9] performed a numerical simulation about natural convection in a two- dimensional cavity filled with an electrically conducting fluid in the presence of a magnetic field aligned to gravity. They selected both Grashof and Hartmann numbers as controlling parameters to examine the effect of a magnetic field on free convection and associated flow dynamics.

The study of heat transfer near irregular surfaces is of fundamental importance; that is because it is often met in many practical applications and devices such as flat-plate solar collectors and flat-plate condensers in refrigerators. The presence of roughness elements disturbs the flow past surfaces and alters the heat transfer rate. Yao [10] examined the natural convection heat transfer from isothermal vertical wavy surfaces, such as sinusoidal surfaces, in Newtonian fluids. He proposed a simple transformation to study the natural convection heat transfer from isothermal vertical wavy surfaces. Hady *et al.* [11] analyzed the problem of MHD free convection flow along a vertical wavy surface in presence of magnetic field and generation absorption. Berrahil and Bessaih [12] studied the magnetohydrodynamics stability oscillatory natural convection in a cylindrical enclosure filled with liquid metal whose Prandtl number equals to 0.015, having an aspect ratio equals to 2, and subjected to an axial temperature gradient and a constant magnetic field. The finite volume method was used in order to solve the governing equations. The results showed the dependence of the critical Grashof number with the increase of the Hartmann number. Ece and Buyuk [13] carried out numerical study of steady, laminer natural convection flow in the presence of a magnetic field in an inclined rectangular enclosure heated from one side and cooled from the adjacent side. The results showed that the orientation and the aspect ratio of the enclosure and the strength and the direction of the magnetic field had significant effects on the flow and temperature fields. They concluded that the circulation inside the enclosure became stronger as the Grashof number increased, while the magnetic field suppressed the convective flow and the heat transfer rate. Al-Najem *et al.* [14] numerically investigated the effect of the transverse magnetic field on flow field patterns and heat transfer processes in a tilted square cavity. The horizontal walls of the enclosure were considered to be insulated while the vertical walls were kept isothermal. The power law control volume approach was developed to solve the conservation equations at Prandtl number of 0.71. The study covered the range of the Hartmann number from 0 to 100, the enclosure inclination angle from 0° to -90° with Grashof number of 10^4 and 10^6. The effect of the magnetic field was found to suppress the convection currents and heat transfer inside the cavity. This effect was significant for low inclination angles and high Grashof numbers. Additionally, it was noted that there was no variation of average Nusselt number with respect to inclination angle for high Hartmann number.

2. MATHEMATICAL FORMULATION

We consider a two-dimensional magneto-hydrodynamic convective flow in an inclined sinusoidal corrugated square enclosure of length W filled with an electrically conducting fluid is considered. The fluid properties are also assumed to be constant, except for the density in the buoyancy term, which follows the Boussinesq approximation. The gravity acts vertically downwards. A uniform external magnetic field B_o is applied perpendicularly to the left side wall. The viscous incompressible flow and the temperature distribution inside the enclosure are described by the continuity and the energy equations, respectively. Under the above assumptions, the governing equations in terms of non-dimensional form as follows:

$$\frac{\partial U}{\partial X}+\frac{\partial V}{\partial Y}=0 \tag{1}$$

$$U\frac{\partial U}{\partial X}+V\frac{\partial U}{\partial Y}=-\frac{\partial P}{\partial X}+Pr\left(\frac{\partial^2 U}{\partial X^2}+\frac{\partial^2 U}{\partial Y^2}\right)+Ra\,Pr\,\theta\,sin(\Phi) \tag{2}$$

$$U\frac{\partial V}{\partial X}+V\frac{\partial V}{\partial Y}=-\frac{\partial P}{\partial Y}+Pr\left(\frac{\partial^2 V}{\partial X^2}+\frac{\partial^2 V}{\partial Y^2}\right)+Ra\,Pr\,\theta\,cos(\Phi)-Ha^2\,Pr\,V \tag{3}$$

$$U\frac{\partial \theta}{\partial X}+V\frac{\partial \theta}{\partial Y}=\frac{\partial^2 \theta}{\partial X^2}+\frac{\partial^2 \theta}{\partial Y^2} \tag{4}$$

where U and V are the dimensionless velocity components in the X and Y directions, respectively, θ is the dimensionless temperature, P is the non-dimensional pressure. The effect of the electromagnetic field is introduced into the momentum equations (3)-(4) through the Hartmann number (Ha) which is defined as:

$$Ha=B_o W\sqrt{\frac{\sigma_e}{\mu}}$$

where σ_e is the electrical conductivity and μ is the dynamic viscosity. The other two important non-dimensional governing parameters appeared in Eqs. (2) and (3) are the Rayleigh number (Ra) and the Prandtl number (Pr) respectively and they are defined as:

$$Ra=\frac{g\beta qW^4}{k\upsilon\alpha} \qquad \text{and} \qquad Pr=\frac{\upsilon}{\alpha}$$

where k is the thermal conductivity of the fluid, g is the gravitational acceleration, β is the volumetric coefficient of thermal expansion, υ is the kinematic viscosity and α is the thermal diffusivity. The dimensionless parameters used in the governing equations (1-4) are expressed in the following forms:

$$X=\frac{x}{W},Y=\frac{y}{W},U=\frac{uW}{\alpha},V=\frac{vW}{\alpha},P=\frac{pW^2}{\rho\alpha^2},\theta=\frac{T-T_c}{(qW/k)}$$

Non-dimensional forms of the boundary conditions for the present problem are specified as follows:

All walls: $U=0$, $V=0$, Top wall: $\dfrac{\partial\theta}{\partial Y}=0,$ Right and left side walls: $\theta=0$,

Bottom wall: $\dfrac{\partial\theta}{\partial Y}=\begin{cases}0 & for \quad 0<X<0.5(1-\varepsilon) \ and \ \ 0.5(1+\varepsilon)<X<1\\ -1 & for \quad 0.5(1-\varepsilon)\le X\le 0.5(1+\varepsilon)\end{cases}$

The averaged Nusselt number (Nu) at the heated surface can be written as (Saha *et al.* [19]):

$$Nu=\frac{1}{\varepsilon}\int_0^{\varepsilon}\frac{1}{\theta_S(X)}dX$$

where $\theta_s(X)$ is the local dimensionless temperature of the heated surface, The Simpson's 1/3 rule is used for numerical integration to obtain the average Nusselt number.

3. NUMERICAL PROCEDURE

The governing differential equations have been solved by Galerkin finite element method. The solution domain is first subdivided into a finite number of grid points. The grid generation calculation is applied to fluid flow. In the present work, eight combinations (40 × 40, 50 × 50, 60 × 60, 70 × 70, 80 × 80, 100 × 100, 120 × 120 and 150 × 150) of non-uniform grids are used to test the effect of grid size on the accuracy of the predicted results. The SIMPLE algorithm is chosen to numerically solve the

governing differential equations in their primitive form. The pressure correction equation is derived from the continuity equation to enforce the local mass balance. First, the momentum equations, Eqs. (2-3) are discretized and linearized. Central differencing is used to discretize the diffusion terms, whereas a blending of upwind and central differencing is used for the convection terms. The source terms in the governing transport equations are functions of the respective transported variables and are calculated implicitly. Linear interpolation and numerical differentiation are used to express the cell-face value of the variables and their derivatives through the nodal values. Discretized momentum equations lead to an algebraic system of equations for velocity components U and V where pressure, temperature, fluid properties are taken from the previous iteration except the first iteration where initial conditions are applied. These linear equation systems are solved iteratively to obtain an improved estimate of velocity. The improved velocity field is then used to estimate new mass fluxes, which satisfy the continuity equation. The pressure-correction equation is then solved using the same linear equation solver and the same tolerance. The energy equation is then solved in the same manner to obtain a better estimate of the new solution.

4. RESULTS AND DISCUSSION

In this research, a numerical study is carried out numerically for different discrete heat source size ratios ε = 0.2, 0.4, 0.6 and 0.8, inclination angles of the sinusoidal corrugated enclosure Φ = 0º, 15º, 30º and 45º, Rayleigh number, $Ra = 10^3$, 10^4, 10^5 and 10^6 and Hartmann number, Ha = 0, 25, 50, 75 and 100.

The result in the form of streamline and temperature are shown in Figs. 2 and 3 for various values of Rayleigh number Ra from 103 to 106 and Hartmann number Ha from 0 to 100 with a discrete heat source size ratio of 0.2 and with constant inclination angle of the sinusoidal corrugated enclosure Φ = 0º. Since the temperature fields are almost symmetric about the vertical mid-plane of the enclosure, whenever the flow fields are asymmetric due to wavy sidewalls. The symmetrical boundary conditions in the vertical direction cause to produce a couple of asymmetrical anticlockwise and clockwise rotating cells in the left and the right halves of the enclosure. In most of the cases, the flow rises along the vertical center line from the middle part of the bottom wall and gets blocked at the top adiabatic wall, which turns the flow horizontally towards the isothermal cold sidewalls. After that, the flow moves downwards along the sinusoidal corrugated sidewalls and turns back horizontally to the central region after hitting the bottom wall. With the increase of Hartmann number, the viscous forces become more dominant than the buoyancy forces and the inner of the two symmetrical circulating cells of almost equal strength is directed towards the end points of the heat source. The isotherm graphs are nearly symmetric about the vertical centre line of the enclosure and the shape of the streamlines tend to follow the geometry of the enclosure as shown in Fig. 3; so heat transfer is essentially diffusion dominated. The temperature decreases from the bottom hot wall to the top adiabatic wall along the vertical centre line of the enclosure and concentrates towards the hot bottom wall indicating the existence of a large temperature gradient. Near the sidewalls of the enclosure, the isotherms are almost symmetrical, while the isotherms in the middle of the enclosure take the shape of smooth curves which are symmetric with respect to the vertical mid-plane of the enclosure. For high Rayleigh number, where buoyancy forces are more dominant than the viscous forces, the convection currents inside the enclosure become very strong. Since the cold fluid has a downward motion with an increase of circular flow, the convection becomes the basic mode of heat transfer. In this case, the anticlockwise and the clockwise rotating cells move up and become irregular in shape. Also, the isotherm pattern changes significantly. With the increase of Rayleigh number, the developing thermal boundary layer thickness at the bottom wall becomes thinner and thus refers high heat transfer rate.

In the Figs. 4 and 5, the result in the form of streamline and temperature are shown for various heat source size ratio (ε) of 0.2, 0.4, 0.6 and 0.8 with different values inclination angles Φ = 0º, 15º, 30º and 45º while the fixed $Ra = 10^6$ and Ha = 0. When Φ = 0º and ε = 0.2. When the inclination angle increases from 0º to 15º, the minor cell at lower right corner becomes smaller and further increases of tilt angle eventually allows the main circulating cell to be dominant. This results in higher recirculation strength and convection current becomes the dominant mode of heat transfer. The flow field is affected by a large rotating cell and becomes identical irrespective of discrete heat source size ratio with the high value of Ra and zero magnetic effect. Now when the heat source size increases, the small clockwise rotating cell at the lower left corner expands, thus squeezing the small right circulating cell. At the inclination angle of 45º, the large circulating cell covers most parts of the sinusoidal corrugated enclosure with a large magnitude of circulation which indicates increasing the buoyancy effect. It then becomes dominating near the heat source while the small right circulating cell decreases in size and in general allows the main flow to move closer to the heat source. Moreover, at Φ = 45º a small minor cell is observed at the top corner of the left cold sidewall and the overall pattern of the stream lines on the upper part of the cavity is same as shown in Fig. 4. The angle of inclination as well as discrete heat source size ratio has noticeable effect on the heat transfer characteristics as shown in Fig. 5. At high Rayleigh and zero Hartmann number, the isotherm plots with temperature contours, $\theta = 0 - 0.03$ occur asymmetrical about the vertical mid-plane of the enclosure. For low inclination angle ($\Phi \leq 15$º) and ε = 0.2, the temperature contours noticeably θ = 0.02 move slightly from left to right and with the increase of inclination angle ($\Phi \geq 30$º), the isotherms are pushed towards the lower part of the right sidewall due to the expansion of main circulating cell. This behavior can be noticed at high heat source size ratio with different inclination

angles. When $\varepsilon = 0.8$, the temperature contours are continuously compressed towards the cold right sidewall. As the non-linearity of the isotherms increases, the existence of a thin thermal boundary layer clusters near the lower part of the right sidewall with the increase of Φ.

The variation of the average Nusselt numbers along the heated strip at the bottom wall with Rayleigh number from 10^3 to 10^6 for different values of Hartmann number, discrete heat source size ratio and enclosure inclination angle are shown in Figs. 6(a), (b) and (c) respectively. From these figures, it is observed that at any particular corrugated geometry with or without the presence of magnetic field, the average Nusselt number does not change up to $Ra = 10^4$ and then it increases significantly with the increasing of Rayleigh number due to convection dominated heat transfer. It is observed that there is no variation of average Nusselt number until $Ra = 10^5$ for $Ha \geq 50$. The effects of discrete heat source size ratio on Nu without the presence of magnetic field ($Ha = 0$) at an inclination angle of 45º is presented in Fig. 6(b). It is also observed that the heat transfer rate decreases with the increase of heat source size and the smaller size ratio produces the maximum value of Nusselt number for any value of Rayleigh number. It is also concluded from Fig. 6(c) that the average Nusselt number significantly increases as the inclination angle increases to a certain value for low Rayleigh number. When the Rayleigh number increases from 10^4 to 10^6, the rate of increase of Nu with the change of inclination angles drops drastically.

5. CONCLUSIONS

The effect of cavity inclination angle, longitudinal magnetic field and discrete isoflux heat source size on natural convection inside a sinusoidal corrugated enclosure are investigated and analyzed in this study. The finite volume method helps to obtain numerical solution in terms of stream functions and temperature contours for $Ra = 10^3$ to 10^6 and $Pr = 0.02$. From the above discussion, following conclusions can be drawn:

(i) The application of a longitudinal magnetic field results in a force opposite to the flow direction that leads to drag the flow and then reduces the convection currents by reducing the velocities.

(ii) For low Rayleigh number and high Hartmann number, diffusion is the basic mode of heat transfer which results the minimum value of thermal performance from the heated wall. On the other hand, with the increase of Rayleigh number, the thermal boundary layer thickness decreases and it would become thinner when the effect of Hartmann number is going to cease on the flow and the thermal fields. Then convection becomes the main mode of heat transfer which in turns enhances the performance of heat transfer inside the sinusoidal enclosure.

(iii) The average Nusselt number increases significantly with the increase of Rayleigh number and the decrease of Hartmann number and hence a magnetic field can be used as an effective mechanism to control the convection inside an enclosure.

(iv) The average Nusselt number also increases as the discrete heat source size decreases and vice verse. The enclosure inclination angle has a clear effect on the heat transfer process as well. It is found that for small size of discrete heat source, the values of Nu increases significantly as soon as the cavity orientation changes from horizontal to any inclined position. Moreover, the effect of change of inclination angle on heat transfer is only dominant at higher value of Rayleigh number.

REFERENCES:

[1] Teamah, M. A., Hydro-magnetic double-diffusive natural convection in a rectangular enclosure with imposing an inner heat source or sink, *Alexandria Engineering J*. 45 (2006) 401-415.

[2] Braithwaite, D., Beaugnon, E., Tournier, R., Magnetically control-led convection in a paramagnetic fluid, *Nature* 354 (1991) 134-136.

[3] Ostrach, S., Natural convection with combined driving forces, *Physico Chemical Hydrodynamics* 1 (1980) 233–247.

[4] Ozoe, H., Okada, K., The effect of the direction of the external magnetic field on the three-dimensional natural convection in a cubic enclosure, *Int. J. Heat Mass Transfer* 32 (1989) 1939–1953.

[5] Tagawa, T., Shigemitsu, R., Ozoe, H., Magnetizing force modeled and numerically solved for natural convection of air in a cubic enclosure: effect of the direction of the magnetic field, *Int. J. Heat Mass Transfer* 45 (2002) 267–277.

[6] Kaneda, M., Tagawa, T, Ozoe, H., Convection induced by a cuspshaped magnetic field for air in a cube heated from above and cooled from below, *J. Heat Transfer* 124 (2002) 17–25.

[7] Xu, B., Li, B., Stock, D., An experimental study of thermally induced convection of molten gallium in magnetic fields, *Int. J. Heat Mass Transfer* 49 (2006) 2009 –2019.

[8] Seki, M., Kawamura, H., Sanokawa, K., Natural convection of mercury in a magnetic field parallel to the gravity, *J. Heat Transfer* 101 (1979) 227–232.

[9] Rudraiah, N., Barron, R., Venkatachalappa, M., Subbaraya, C., Effect of a magnetic field on free convection in a rectangular enclosure, *Int. J. Engng. Sci.* 33(8) (1995) 1075–1084.

[10] Yao, L., Natural convection along a vertical wavy surface, J. Heat Transfer 105 (1983) 465-468.

[11] Hady, F., Mohamed, R., Mahdy, A., MHD free convection flow along a vertical wavy surface with heat generation or absorption effect, *Int. Comm. Heat Mass Transfer* 33 (2006) 1253-1263.
[12] Berrahil, F., Bessaih, R., Magnetohydrodynamic stability of oscillatory natural convection in a cylindrical enclosure filled with liquid metal, *World J. Engg*. 5 (2008) 1-9.
[13] . Ece, M, Buyuk, E., Natural convection flow under a magnetic field in an inclined rectangular enclosure heated and cooled on adjacent walls, *Fluid Dynamics Research* 38 (2006) 546-590.
[14] Al-Najem, N., Khanafer, K., M., Numerical study of laminar natural convection in tilted enclosure with transverse magnetic field, *Int. J. Numerical Methods Heat Fluid Flow* 8(6) (1998) 651-672.

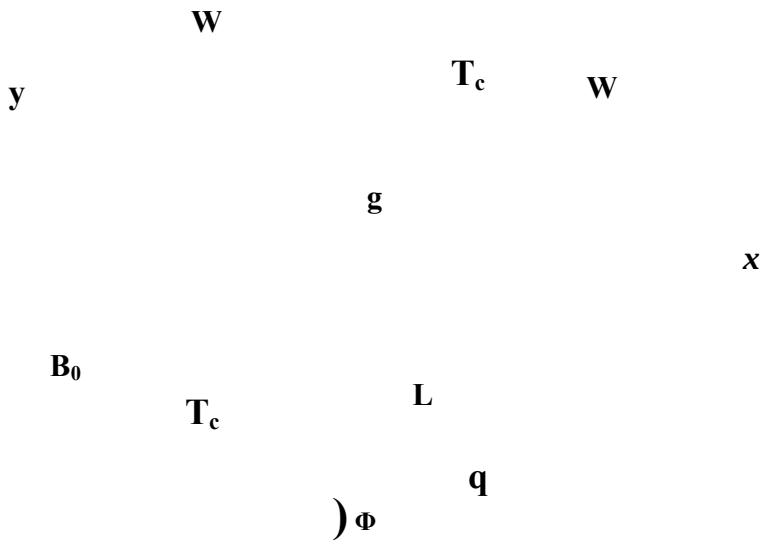

Figure 1: Schematic of the dimensional physical problem considered

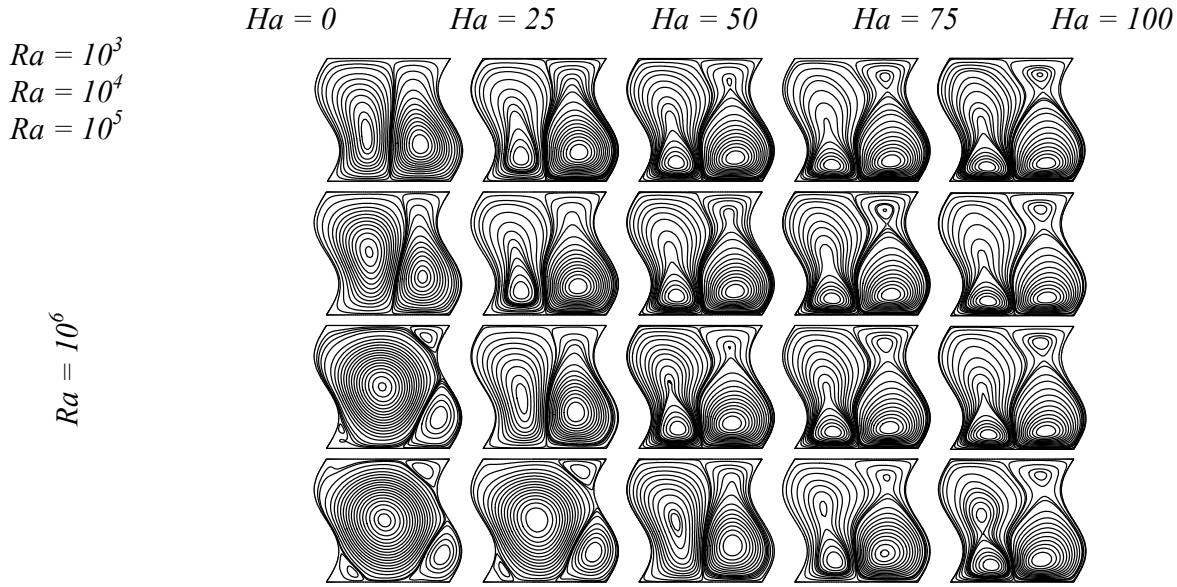

Figure 2: Streamlines for different Hartmann numbers (*Ha*) and Rayleigh numbers (*Ra*) with $\varepsilon = 0.2$ and $\Phi = 0^o$

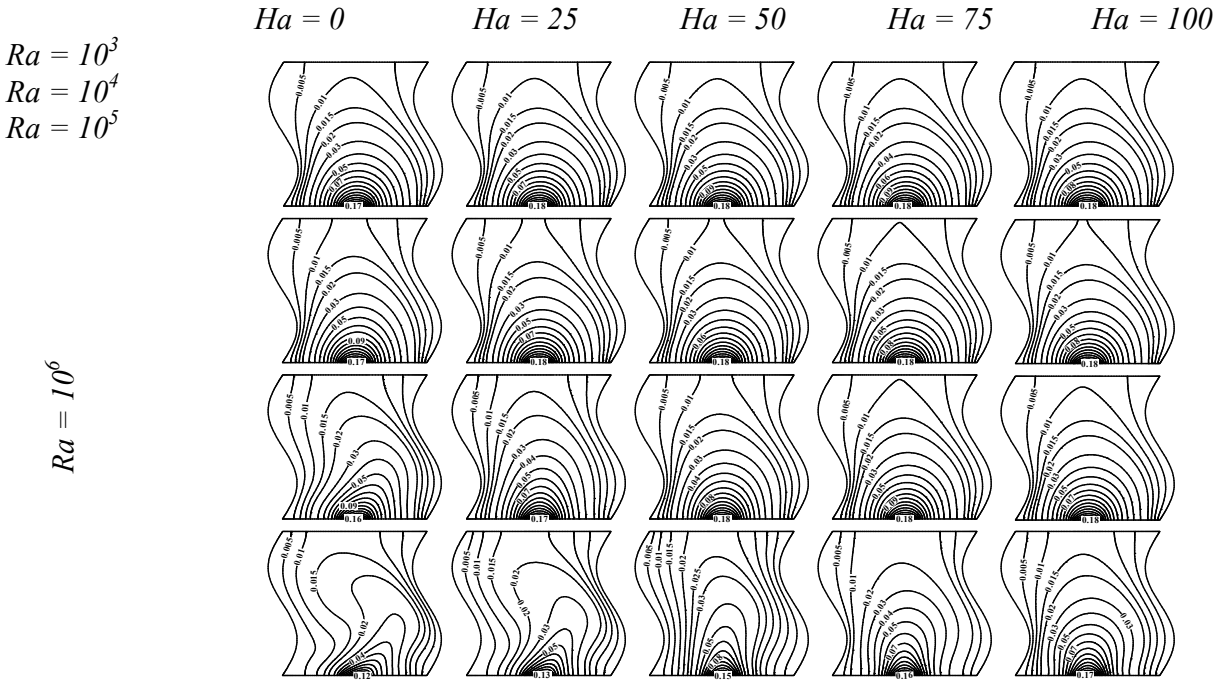

Figure 3: Isotherms for different Hartmann numbers (*Ha*) and Rayleigh numbers (*Ra*) with $\varepsilon = 0.2$ and $\Phi = 0^o$

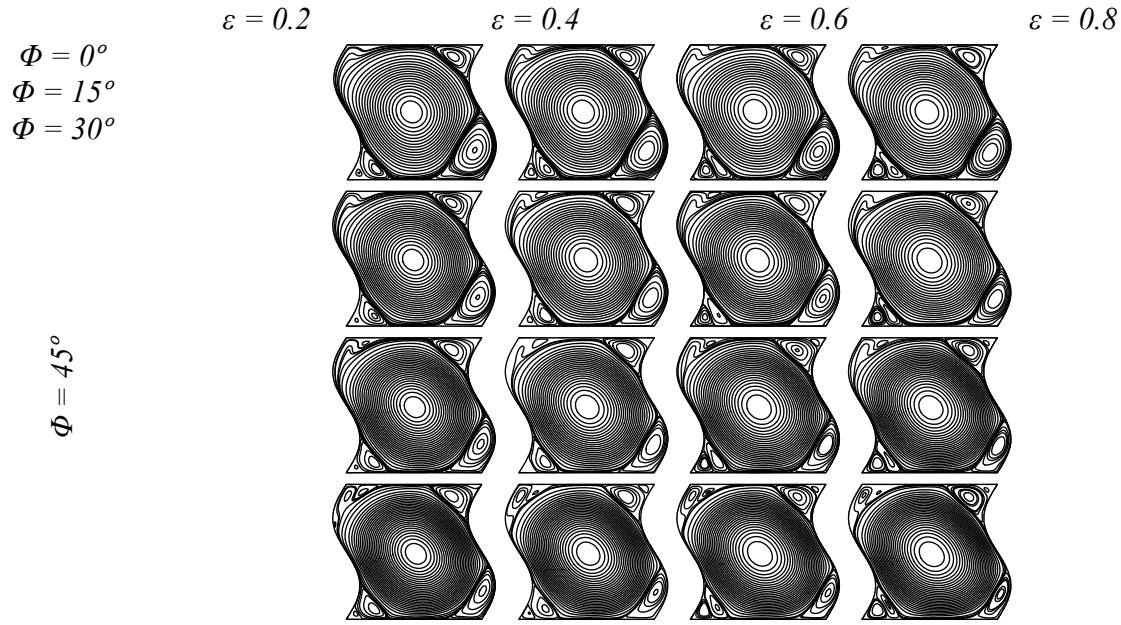

Figure 4: Streamlines for different discrete heat source size ratios (ε) and inclination angles (Φ) with $Ha = 0$ and $Ra = 10^6$

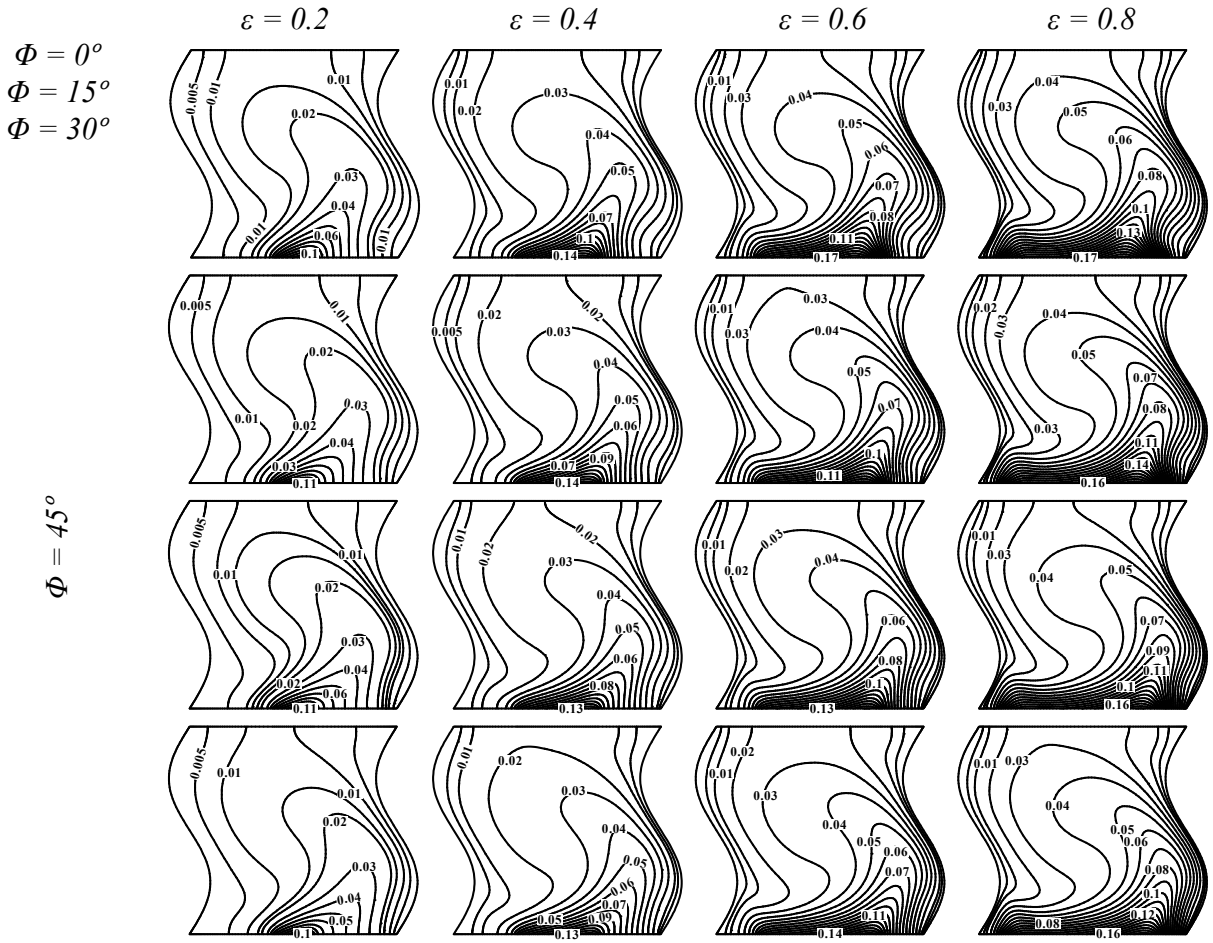

Figure 5: Isotherms for different discrete heat source size ratios (ε) and inclination angles (Φ) with $Ha = 0$ and $Ra = 10^6$

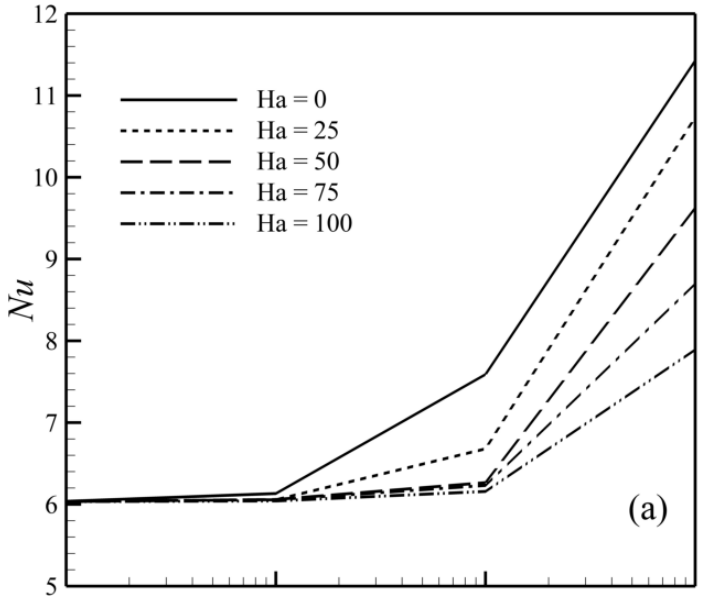

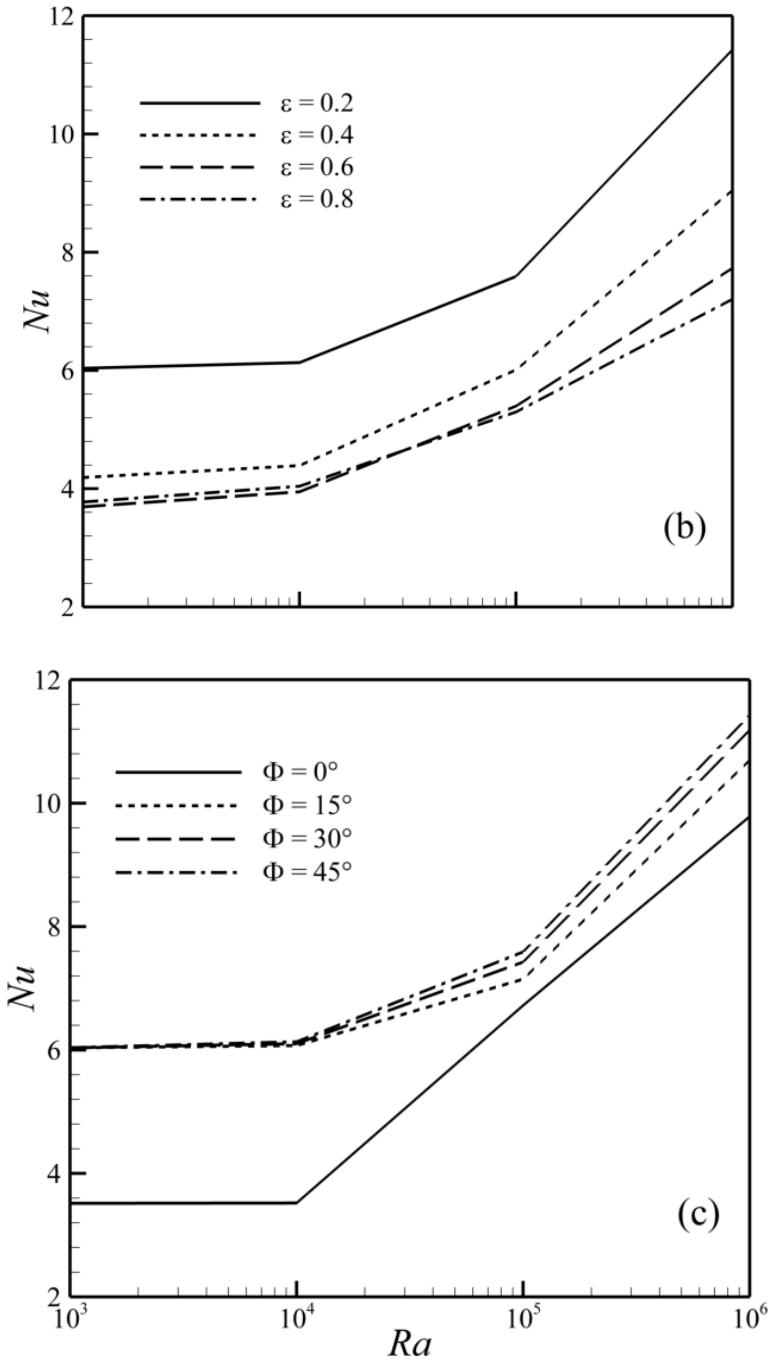

Figure 6: Variation of the average Nusselt number (*Nu*)